JOURNAL OF MATERIALS SCIENCE 29 (1994) 4385–4392

Creep of porcelain-containing silica and alumina

R. PONRAJ, S. RAMAKRISHNA IYER and V. M. RADHAKRISHNAN
Department of Metallurgical Engineering, Indian Institute of Technology, Madras 600 036, India

Hard porcelain ceramics find many applications because of their high hardness, high mechanical strength and moderate thermal-shock resistance. The addition of alumina as a filler to porcelain increases its strength at room temperature. In the present investigation, four-point-bend creep tests were carried out for porcelain-containing silica (SP-1) and alumina (AP-3) at 800, 900 and 1000 °C. The creep data were analysed using a power-law creep, and the stress exponents were estimated. The activation energy for these two materials was found to be 45 kcal mol^{-1}. The viscosity of the feldspar glassy phase was also determined from the creep tests. The test samples were analysed by scanning electron microscopy (SEM). The X-ray diffraction results (XRD) show that the amount of crystalline phase in the material increases after creep testing.

1. Introduction

The study of creep properties of ceramics will improve the understanding of the contributions of their various constituents to deformation processes. For a material like porcelain which contains about a 50% glassy phase, the deformation mechanism will be entirely different from that in polycrystalline ceramics. Cannon and Langdon [1] have collected creep data for many ceramics.

Many authors have reported that the room-temperature strength of porcelain-containing alumina is better than that containing silica [2]. Further, it is observed that an increase in the alumina content of the glassy phase, as well as in the crystalline form, reduces the number of microcracks in the fired body and the strength of the porcelain is thus increased. Dunsmore *et al.* [3] studied the high-temperature mechanical properties of two porcelains – a chemical porcelain with a high-silica content and a refractory porcelain with a high-alumina content. They concluded that mullite formed in the aluminous porcelain increases the strength. Salmang [4] has found that the alumina content in porcelain raises the onset of softening (compared to normal glass).

Chaudhuri [5] has reported the short-time creep properties of siliceous porcelain in a relatively narrow range of temperature from 1075 to 1125 °C. He estimated the thermal activation energies of creep and viscous flow of the glassy phase and found that both are almost the same. Based on these studies, he concluded that the glassy phase increases the creep characteristics of porcelain strongly. However, not much work has been done on the creep properties of hard porcelain with long exposure times in the temperature range 800–1000 °C. Parmalee and Badger [6] have compared the viscosities of porcelain bodies in the temperature range 690–885 °C by loading previously fired rods in torsion. According to most workers [4, 5, 7, 8], the glassy matrix in the body is primarily responsible for the creep or flow behaviour, while the crystalline phases influence the creep of the body by increasing the apparent viscosity of the matrix.

The objective of the present investigation was to study the creep properties of porcelains containing alumina and silica in the temperature range 800–1000 °C.

2. Experimental procedure

2.1. Sample preparation

Two types of commercial electrical-grade porcelains were supplied by W. S. Industries (India), namely, (i) siliceous porcelain (SP-1) containing a standard composition of 50 wt % clay, 25 wt % potassium feldspar and 23 wt % silica as filler; and (ii) aluminous porcelain (AP-3) containing 45 wt % clay, 25 wt % potassium feldspar and 30 wt % alumina as filler.

The SP-1 and AP-3 bodies were prepared by the following steps. The raw materials in the form of powder were weighed and mixed with a suitable amount of water and then ground in a ball mill. The resulting slurry or slip consisted of fine raw materials suspended in a water media. The water in the slip was removed in a filter press, resulting in a cake formation which was suitable for extrusion. A vacuum pug mill extrusion machine was used to produce rectangular bars of dimensions 12×25 mm^2 and a length of about 150 mm. The water content of the extruded bodies was further reduced by drying them in an oven maintained at 100 °C for 12 h.

0022–2461

2.2. Creep test

Samples for four-point creep testing were prepared from those dried samples which had good green strengths. The creep specimens were $3.5 \times 4.5 \times 50\ mm^3$. The final surface was prepared using fine-grade-silicon-carbide emery papers. These samples were fired in a production kiln at a temperature of 1250 °C.

A four-point-bend creep-testing unit was designed and fabricated for this investigation; the details are reported elsewhere [9]. The loading fixture, with the test specimen in position, is shown in Fig. 1. The loading and supporting blocks were made out of silicon carbide (supplied by Carborundum Universal Ltd., Madras), with inner and outer spans of 20 and 40 mm, respectively. The load was applied to the specimens by an alumina tube which rested on the loading block. The loading assembly was supported by a lever with a counterweight which rested on a fulcrum. The sample was heated by an electrical furnace having four kanthal coils arranged parallel to the specimen length. In the upper loading block a reference mark, about $3 \times 3\ mm^2$ in size, was provided on the bottom side which just touched the upper portion of the specimen. As the specimen bent during creep, the distance between the specimen and the reference mark increased and this was measured using a travelling microscope through a front window in the furnace assembly. Illumination provided at the back side of the furnace increased the contrast between the reference mark and the upper side of the specimen, which enabled the measurement to be made accurately. The deflection was continuously measured with respect to time allowing calculation of the outer fibre strain using the formula

$$\varepsilon = \frac{6hd}{(L - a)(L + 2a)} \quad (1)$$

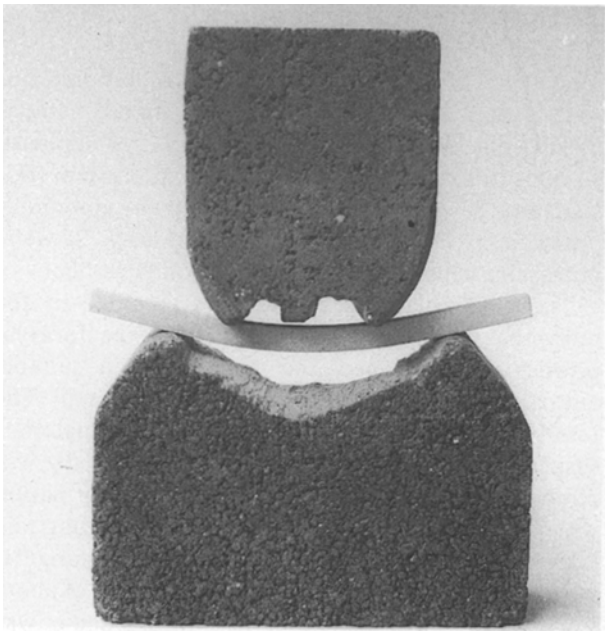

Figure 1 A four-point-bend creep-testing fixture made of silicon carbide with the creep-tested sample in position.

The maximum outer fibre stress, σ, was obtained from the expression

$$\sigma = \frac{3(L - a)P}{2bh^2} \quad (2)$$

where L is the outer span length, a is the inner span length, P is the load, b is the specimen breadth, h is the specimen width, d is the deflection in the specimen, ε is the maximum outer fibre strain, and σ is the maximum outer fibre stress.

The maximum strain was restricted to about 2%. The tests were carried out at specimen temperatures of 800, 900 and 1000 °C.

Since the porcelain contained large amounts of glassy phase at high temperatures, it formed a viscous liquid and most of the high-temperature properties are based on this phase. Hence the viscosity of the feldspatic glass was estimated from the creep-test data using the following equation [10],

$$\eta = \frac{\sigma}{3\dot{\varepsilon}_s} \quad (3)$$

where η is the viscosity (Pa s), σ is the stress, and $\dot{\varepsilon}_s$ is the minimum creep rate (s^{-1}).

2.3. Microstructural studies

Both optical and scanning electron microscopy (SEM) were used to investigate the microstructural features of porcelain samples SP-1 and AP-3 before and after creep testing. The sample preparation for optical microscopy involved the usual metallographic techniques, and final polishing was carried out using a 0.3 μm alumina slurry in a water medium on a disc polishing cloth. After producing a mirror finish, a 5% HF solution was used to etch the surface and this resulted in selective removal of glassy phase alone leaving all the crystalline phases.

The scanning electron microscope used in this study was a Jeol (Japanese) make. Broken surfaces of the crept samples in the etched and unetched conditions were observed by SEM after giving them a gold-sputter coating. A 5% HF solution was also used for etching these samples.

2.4. Phase analysis by an XRD method

The glassy phase in porcelain is important in determining high-temperature mechanical properties such as the creep resistance. The estimation of the amount of glassy phase in the as-fired specimens was carried out by an internal standard method using X-ray diffraction (XRD). Fine calcium fluoride (CaF_2) was used as the internal standard. A detailed investigation of this technique is reported elsewhere [11] and only a brief outline of the experimental procedure is discussed here. First the total amount of crystalline phases such as quartz, mullite and alumina were evaluated by this technique, and the amount of glassy phase was determined by the difference from 100% of the crystalline phases present. The calibration plots are shown in Fig. 2, using materials with known amounts of crystalline and glassy phases. In ceramic materials like porcelain, the overlapping of prominent

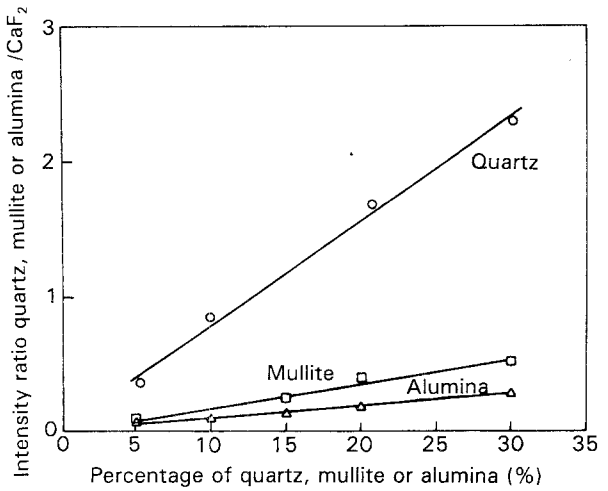

Figure 2 Calibration plots for (△) alumina, (□) mullite and (○) quartz using XRD.

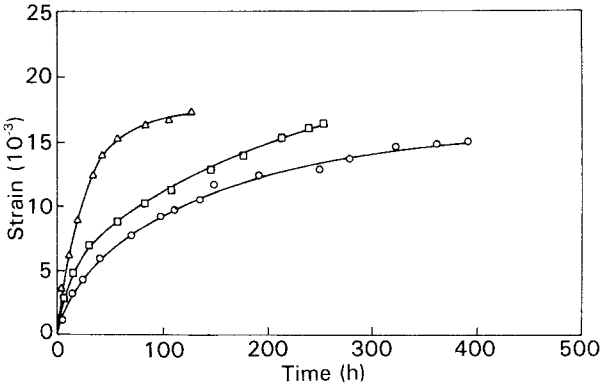

Figure 3 Typical creep curves for AP-3 at 900 °C for the following stress levels: (○) 29 MPa, (□) 36 MPa, (△) 43 MPa.

reflected peaks is a common problem. To solve this problem a computer program was effectively used for the deconvolution of overlapping reflections (with about ± 5% error). The prominent peaks selected are given in Fig. 2, along with their relative intensities, for different crystalline phases. CuK_α radiation was used, and a slow-step scan in the 2θ range 25–30° was carried out.

3. Results and discussion

3.1. Creep analysis

Creep curves generally consist of three stages, namely, primary, secondary and tertiary stages. Fig. 3 shows typical creep curves obtained in bending, for AP-3 at 900 °C at various stress levels. Since the maximum strain and thus the corresponding deflection are restricted in the bending type of creep testing, the creep curves terminate in a steady-state condition and a tertiary stage could not be obtained. The SP-1 material showed a similar creep behaviour to AP-3, but had higher creep rates for the same conditions of temperature and stress.

The steady-state creep rate, $\dot{\varepsilon}_s$, is an important parameter, and it can be expressed as a function of stress and temperature in the form

$$\dot{\varepsilon}_s = A_0 \sigma^n \exp(-Q/RT) \quad (4)$$

$$\dot{\varepsilon}_s = A_1 \sigma^n \quad (5)$$

where A is a constant, A_1 is a temperature-dependent constant, n is a creep stress exponent, Q is an activation energy, R is the gas constant, and T is the temperature in kelvin.

Fig. 4 shows a log–log plot of applied stress and steady-state creep rate for both SP-1 and AP-3. The slope of the lines at a particular temperature gives the stress exponent, n. It can be seen that both materials have almost the same slope in the stress and temperature regions tested. The values of n are 2, 1.62 and 1.54 at 800, 900 and 1000 °C respectively. The n-values in the range 1–2 have been noted for a number of ceramics [1]. The approximately equal values of n for these two types of porcelain at a particular temperature shows that the deformation mechanism was the same in both cases at the given temperature. This observation can be understood on the basis that the porcelains contain about a 50 to 60% glassy phase, and that at high temperatures this glassy phase first reacts and then forms a low-viscosity matrix. The presence of low-viscosity phase in large amounts will control creep behaviour [5, 12]. Cannon and Langdon [1, 13] have compiled creep data for various ceramic materials, and they have noted many ceramics have n-values close to unity.

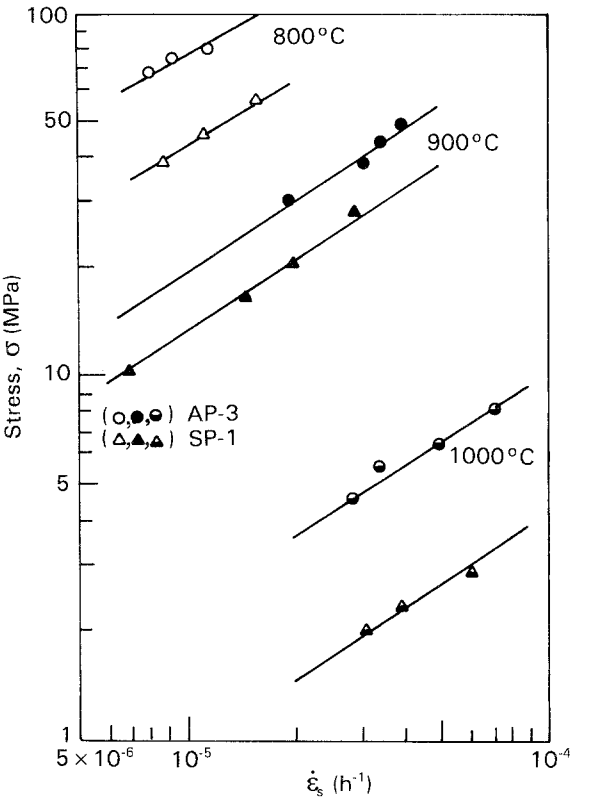

Figure 4 Log–log plot of applied stress and steady-state creep rate for SP-1 and AP-3. At 800 °C, $n = 2$; at 900 °C, $n = 1.64$; and at 1000 °C, $n = 1.54$.

The activation energy has been estimated for AP-3 and SP-1. The constant A_1 in the power-law creep has been computed at different temperatures. The temperature dependence of A_1 is assumed to be of the form

$$A_1 = A_0 \sigma \exp(-Q/RT) \quad (6)$$

Plots of log A_1 versus $1/T$ result in straight lines with slopes equal to $(-Q/R)$. Such plots obtained for SP-1 and AP-3 are shown in Fig. 5. The activation energy, Q, for the materials tested has been found to be 44.4 kcal mol^{-1}. Chaudhuri [5] has calculated the activation energy for hard porcelains in the temperature range 1075–1125 °C and found that it varied between 120 and 287 kcal mol^{-1}. Further he found that the variation in these values is mainly due to the mineralogical composition and microstructure. Davis and Pask [14] estimated the activation energy of the alumino-silicate glassy phase. They found that the activation energy is dependent on the amount Al_2O_3 (wt %) in the system. It is reported that activation energy decreased from 310 to 60 kcal mol^{-1} with an increase in Al_2O_3 from 4 to 22 wt %. The present value of $Q = 45$ kcal mol^{-1} indicates that the creep deformation process is controlled by the glassy phase in both the materials. Further, this low activation-energy value may be due to the nature and composition of the potassium-feldspar glassy phase present in the materials.

A relation between the average creep rate in the primary stage, given in the form ε_{12}/t_{12} (where ε_{12} is the strain up to the first stage and t_{12} is the corresponding time) and the minimum creep rate $\dot{\varepsilon}_s$ can be obtained as

$$\frac{\dot{\varepsilon}_s t_{12}}{\varepsilon_{12}} = \text{constant} \qquad (7)$$

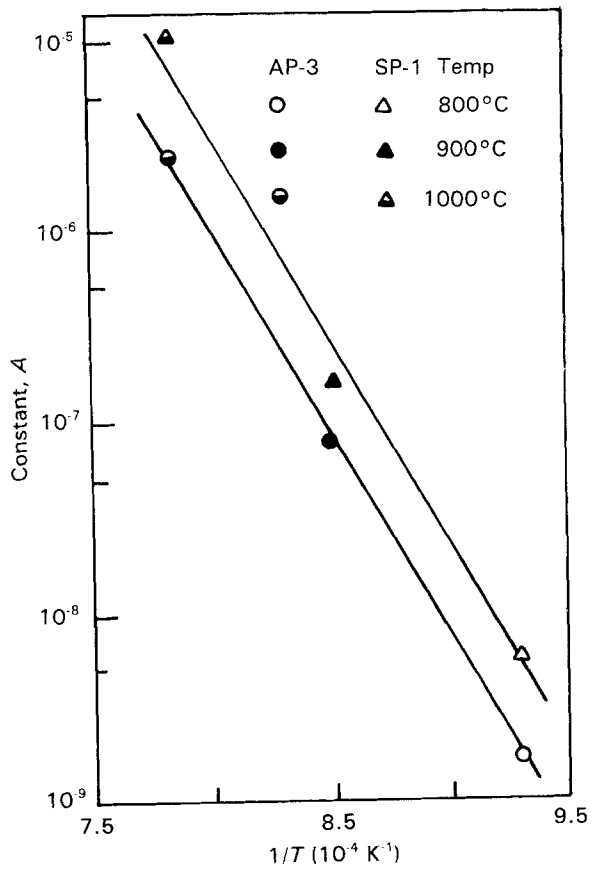

Figure 5 Log A versus $(1/T)$ for SP-1 and AP-3 at different temperatures.

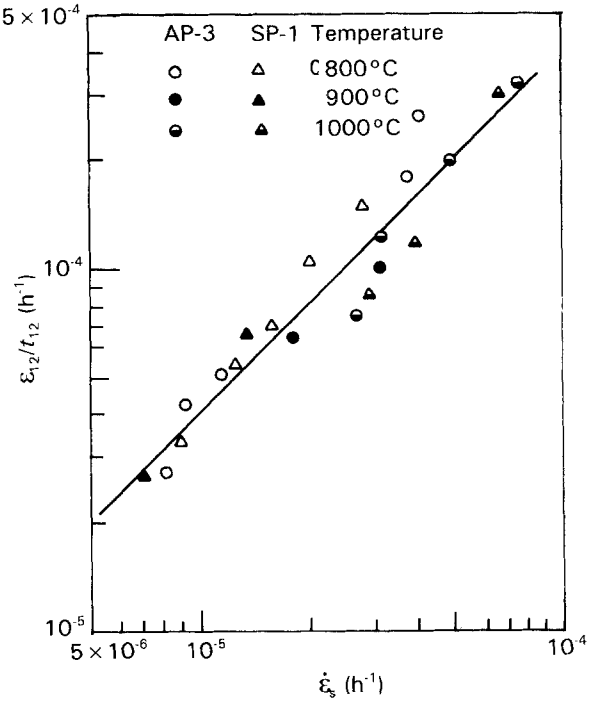

Figure 6 Relation between ε_{12}/t_{12} and the minimum creep rate.

and this equation was found to give a good correlation for metallic materials [15]. In the present study, Equation 7 has been used and the relation between ε_{12}/t_{12} and the minimum creep rate $\dot{\varepsilon}_s$ for SP-1 and AP-3 is shown in Fig. 6. The relation appears to be valid in the case of the ceramics studied in this investigation.

3.2. Microstructural studies

Fig. 7a and b shows the optical microstructures of SP-1 and AP-3 in the as-fired condition. The density of quartz particles was greater in SP-1 than in AP-3. Although no quartz was intentionally added to AP-3, clay and feldspar contain small amounts of quartz. Microcracks were seen in the quartz particles. Crystalline phases, such as mullite and alumina particles, were not apparent in the optical microscopy observations. This is because the mullite was present as needle-shaped particles of submicrometre size. In the case of AP-3, the alumina were also present in the micrometre range and thus it could not be revealed in the microstructures. Thus, the optical-microscope studies of porcelain were limited to an examination of the quartz particles in the glassy matrix. However, Newberger *et al.* [16] have used optical phases with an aluminium sputter coating.

The SEM microstructure of SP-1 in the etched condition is shown in Fig. 8. Crystalline phases, such as quartz and mullite, are seen clearly. The microcracks present in many of the quartz grains are also revealed. Fig. 9 shows a SEM micrograph of AP-3 in the as-fired condition. In addition to quartz and mullite, many alumina particles can also be seen. The alumina particles are smaller than the quartz particles. In addition to mullite needles, alumina-rich regions can also be seen. It can be observed that only a small

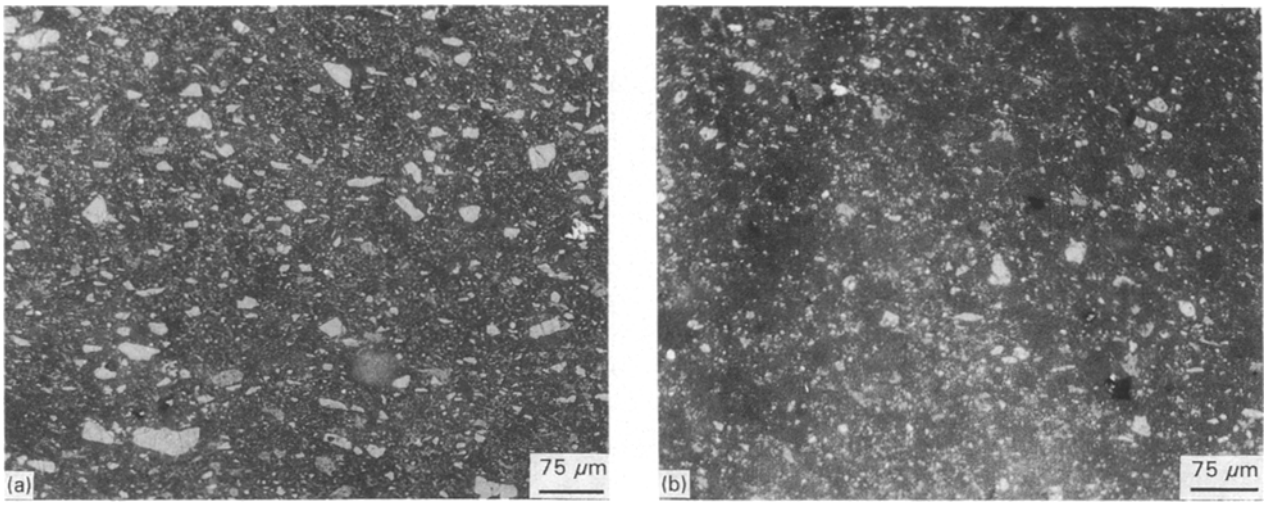

Figure 7 Optical microstructures in the as-fired condition: (a) SP-1, (b) AP-3. Both materials were etched with 5% HF for 5 min at room temperature.

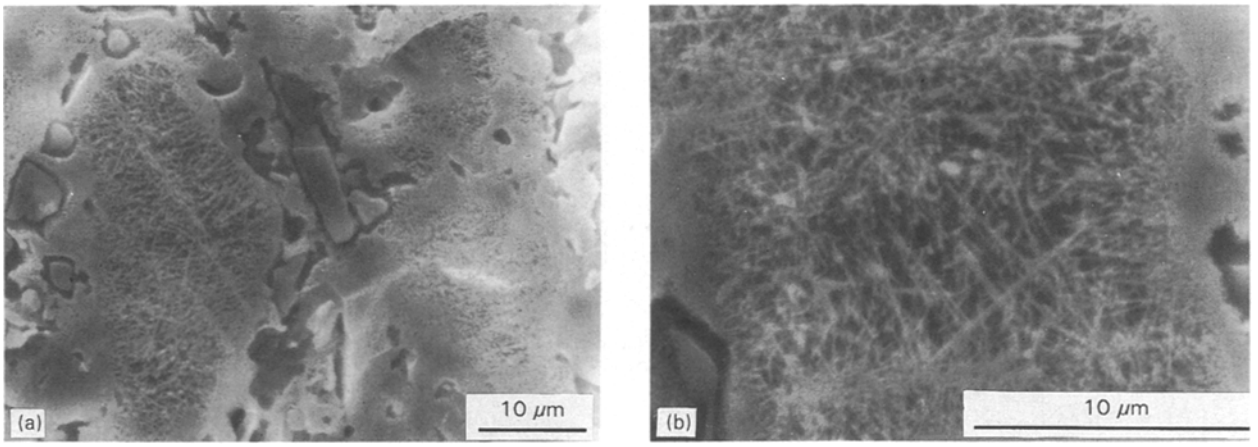

Figure 8 SEM of SP-1 in the as-fired condition after etching in 5% HF: (a) more quartz particles are seen along with mullite in the glassy matrix, and (b) mullite-needle networks.

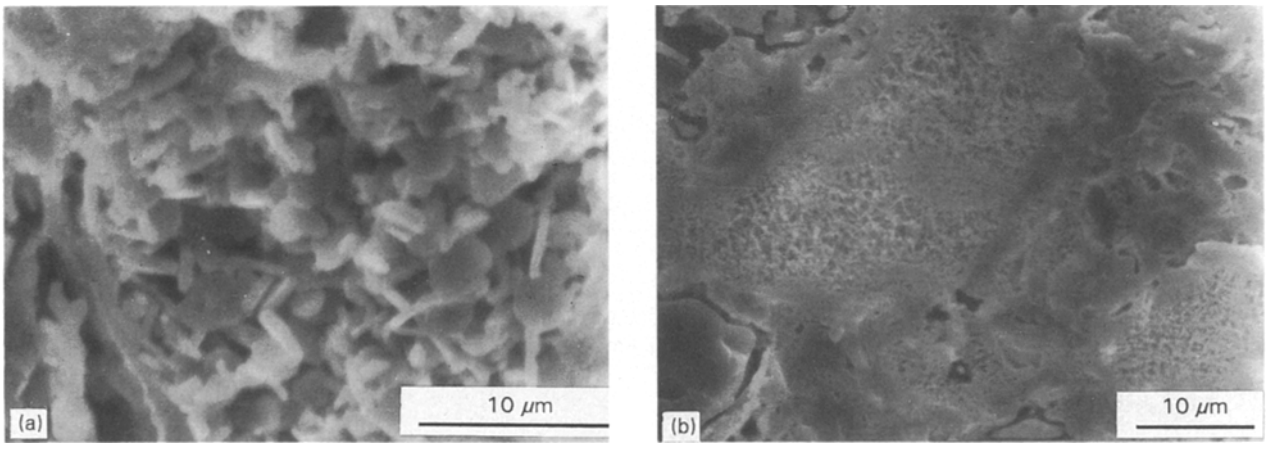

Figure 9 SEM micrograph of AP-3 in the as-fired condition after etching in 5% HF: (a) an alumina-dominated region with some quartz and mullite, and (b) a few quartz particles and mullite networks in a glassy matrix.

number of quartz particles are present in AP-3 compared to SP-1.

SEM micrographs of creep-tested samples at 800, 900 and 1000 °C are given in Figs 10, 11 and 12 respectively, for SP-1 and AP-3. Fig. 13 shows the SEM microstructure of SP-1 and AP-3 samples crept at 1000 °C in the unetched condition. A number of pores can be seen in the deformed matrix. Further, the glassy matrix shows a number of fine cracks in the SP-1 samples. No such cracks are evident in AP-3.

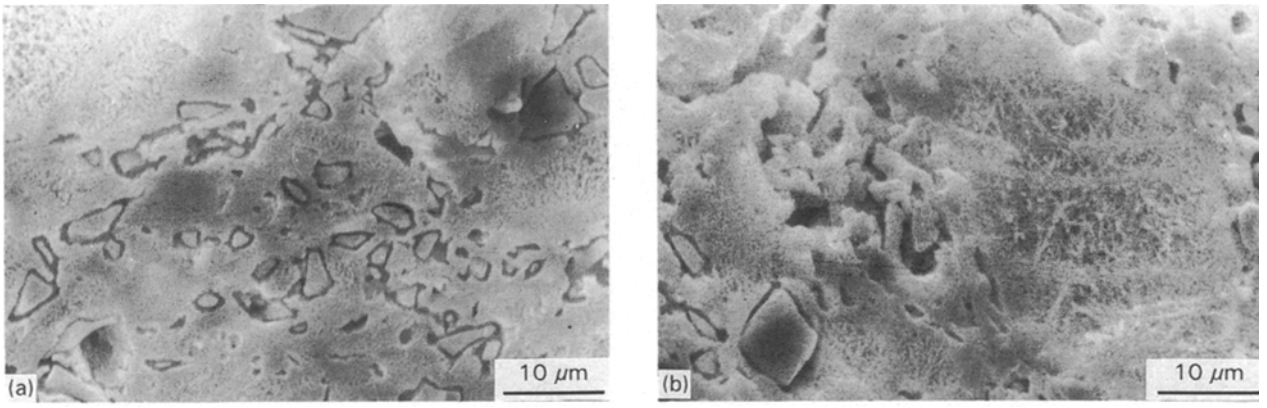

Figure 10 (a) A SEM micrograph of SP-1 after creep testing at 800 °C (stress = 46.60 MPa, time = 500 h), etched with 5% HF. (b) A SEM micrograph of AP-3 after creep testing at 800 °C (stress = 78.50 MPa, time = 500 h), etched with 5% HF.

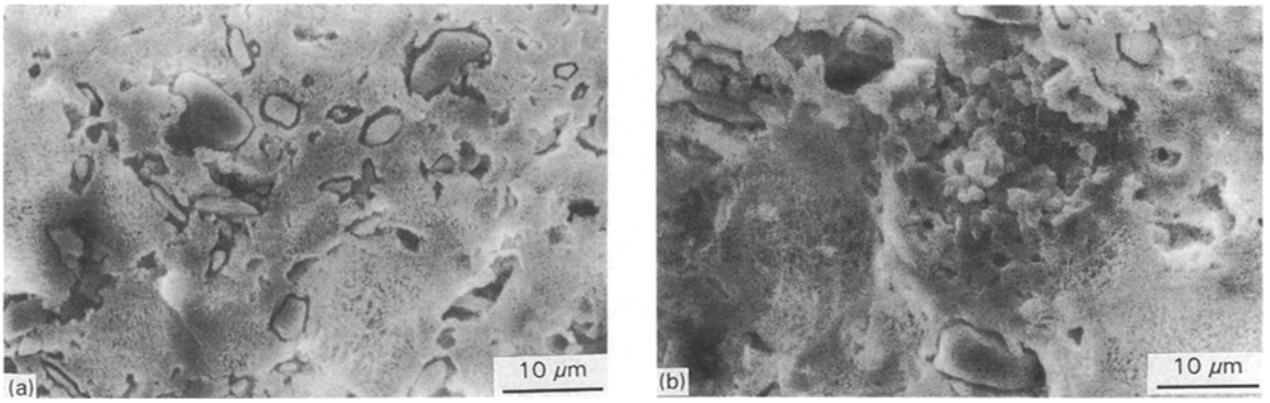

Figure 11 (a) A SEM micrograph of SP-1 after creep testing at 900 °C, (stress = 10.00 MPa, time = 800 h), etched with 5% HF. (b) A SEM micrograph of AP-3 after creep testing at 900 °C, (stress = 29.60 MPa, time = 400 h), etched with 5% HF.

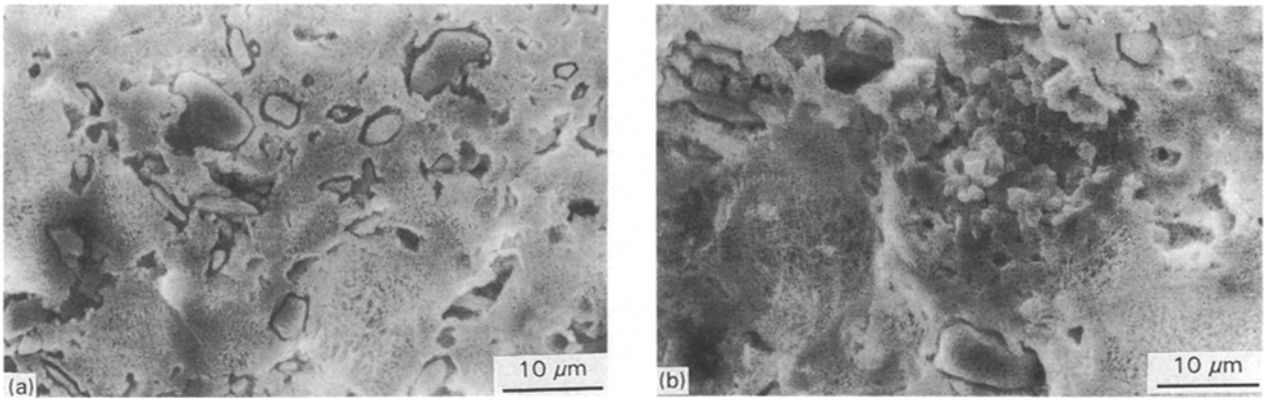

Figure 12 (a) A SEM micrograph of SP-1 after creep testing at 1000 °C (stress = 2.10 MPa, time = 350 h), etched with 5% HF. (b) A SEM micrograph of AP-3 after creep testing at 1000 °C (stress = 4.5 MPa, time = 450 h), etched with 5% HF.

TABLE I Quantitative estimation of the crystalline phases in (SP-1) in the as-fired condition and after creep testing at 800, 900 and 1000 °C

Condition	Quartz (%)	Alumina (%)	Mullite (%)	Glass (%)
As-fired	16.89	4.67	20.87	57.57
800 °C	17.15	4.87	24.28	53.70
900 °C	17.99	6.39	25.05	50.55
1000 °C	14.20	4.92	32.149	48.74

TABLE II Quantitative estimation of the crystalline phases in (AP-3) in the as-fired condition and after creep testing at 800 °C, 900 °C and 1000 °C

Condition	Quartz	Alumina	Mullite	Glass
As-fired	6.89	31.13	15.17	46.81
800 °C	7.80	35.20	14.80	42.20
900 °C	11.27	36.32	15.28	37.13
1000 °C	9.55	39.37	17.48	33.60

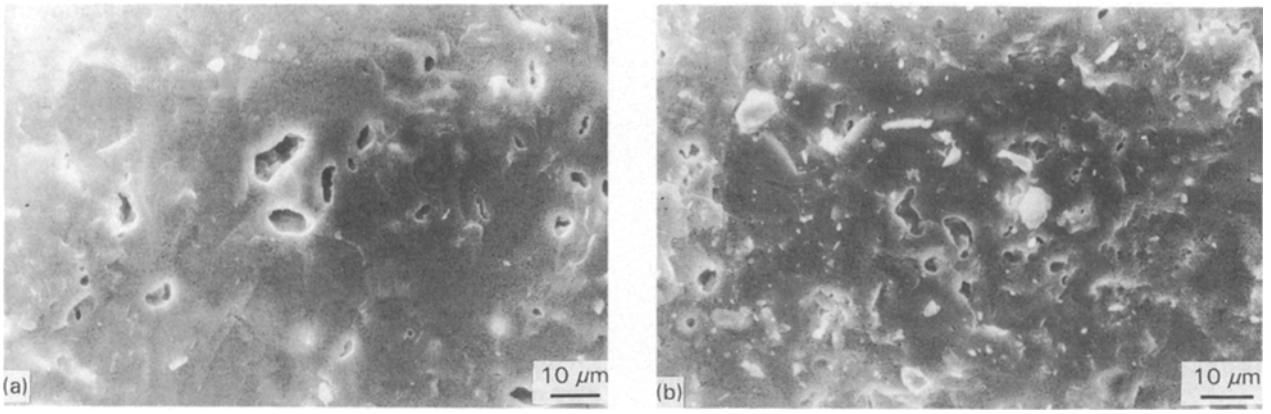

Figure 13 (a) A SEM micrograph of SP-1 after creep testing at 1000 °C (unetched). (b) A SEM micrograph of AP-3 after creep testing at 1000 °C (unetched).

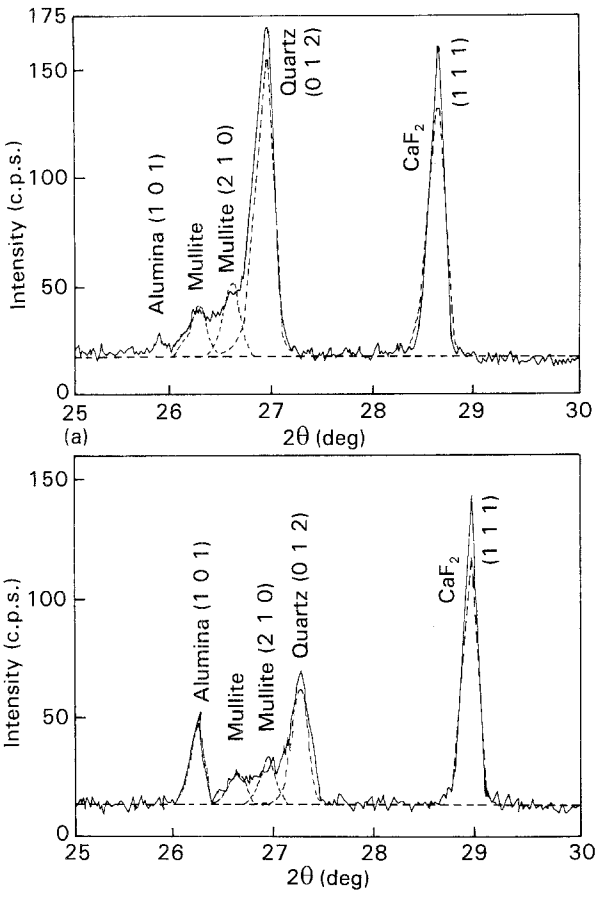

Figure 14 Typical XRD pattern in the as-fired condition of: (a) SP-1, and (b) AP-3. (——) Experimental peaks, and (– – –) peaks after a beam-splitting step.

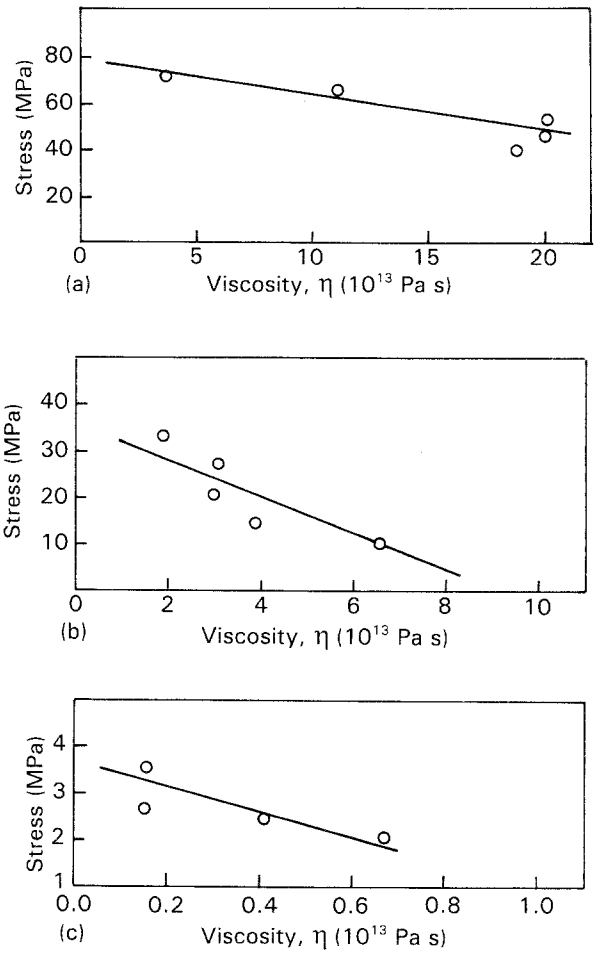

Figure 15 Viscosity of the glassy phase in SP-1 as a function of the applied stress at: (a) 800 °C, (b) 900 °C, and (c) 1000 °C.

The presence of fine alumina, in addition to mullite particles, in AP-3 results in a glassy phase different to that of SP-1.

3.3. Phase analysis

The results of the phase analysis are given in Tables I and II. For SP-1 and AP-3, respectively, before and after creep testing. A typical XRD pattern obtained in the as-fired condition is given in Fig. 14. The results show that there is more mullite formation in the as-fired condition in SP-1 than in AP-3. About a 58% glassy phase is present in SP-1 and a 47% phase in AP-3. Phase analysis in the creep-tested samples generally shows that the amount of crystalline phases increases as the temperature of testing increases; as a result, the volume of the glassy phase reduces.

3.4. Viscosity of glassy phase

The variation in viscosity of SP-1 and AP-3 at the three test temperatures is shown in Figs 15 and 16. The viscosity increases as the stress level decreases. As the temperature increases, the viscosity decreases. The

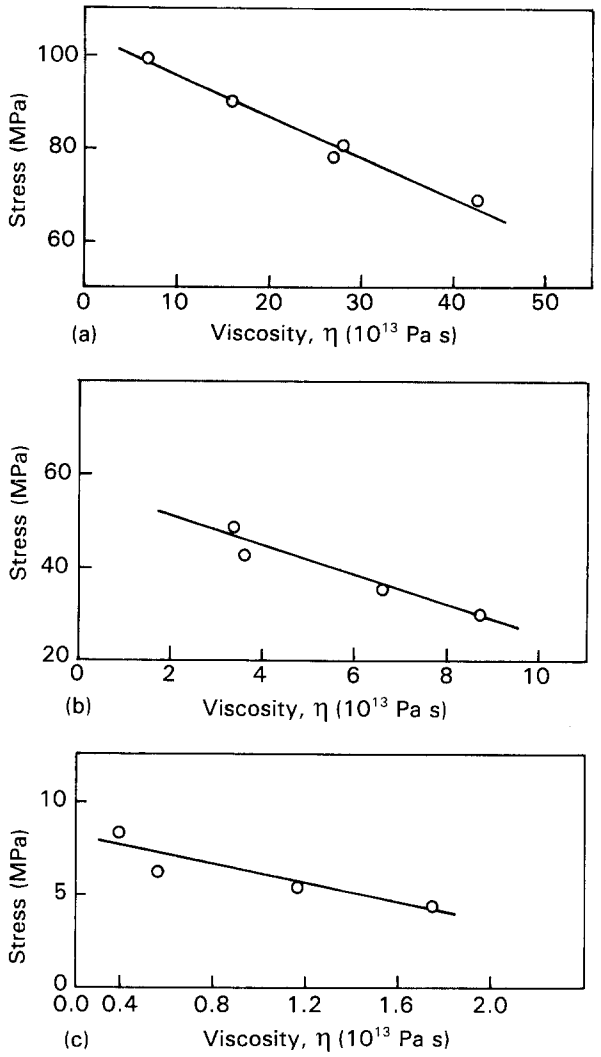

Figure 16 Viscosity of the glassy phase in AP-3 as a function of the applied stress at: (a) 800 °C, (b) 900 °C, and (c) 1000 °C.

magnitude of the viscosity in AP-3 is almost double that in SP-1 for similar test condition; this is consistent with the creep data. SP-1 contains almost 10% more glassy phase than AP-3, which would decrease the viscosity of SP-1 compared to that of AP-3. Also, the presence of alumina in AP-3 would produce a different composition for the glassy phase, which may have also increased the viscosity of the glassy phase.

Salmang [4] has reported that the viscosity of a potash feldspar glass changes logarithmically over the temperature range 1000–1200 °C. Also, Salmang found that the viscosity was increased by the addition of SiO_2, and that small amounts of Al_2O_3 addition lowered the viscosity but large additions raised it again. In the present study, a significant increase in viscosity was observed upon the addition of 30 wt % alumina to porcelain.

4. Conclusions

From the investigations carried to study the creep behaviour of porcelain-containing silica and alumina in the temperature range of 800–1000 °C the following conclusions can be drawn.

1. The creep deformation rate obeys a power-law creep, with the value of the stress exponent, n, equal to 2 at 800 °C. The exponent decreases as the temperature increases.
2. The activation energy for both the materials was found to be 45 kcal mol^{-1}.
3. The creep resistance of AP-3 is higher than that of SP-1 at all test temperatures. The amount of glassy phase in aluminous AP-3 is about 10% lower than in siliceous porcelain SP-1 in the as-fired condition. The presence of more of the glassy phase in SP-1 explains its lower creep resistance compared to AP-3.
4. The viscosity decreases as the temperature is increased or as the stress is increased.
5. The viscosity of AP-3 is almost double that of SP-1, which explains why AP-3 is more creep resistant than SP-1.
6. In both materials, phase analysis by XRD showed a slight increase in the crystalline phases after creep testing.
7. Microvoids and cracks nucleate in the matrix due to creep.

References

1. W. R. CANNON and T. G. LANGDON, *J. Mater. Sci.* **18** (1983) 1.
2. S. K. KHANDELWAL and R. L. COOK, *Amer. Ceram. Soc. Bull.* **49** (1970) 522.
3. G. K. DUNSMORE, J. E. FENSTERMACHER and F. A. HUMMEL, *ibid.* **40** (1961) 310.
4. H. SALMANG, "Ceramics: physical and chemical fundamentals" (Butterworths, London, 1961) p. 329.
5. S. P. CHAUDHURI, *Trans. Indian Ceram. Soc.* **32** (1973) 70.
6. C. W. PARMALEE and A. E. BADGER, *J. Amer. Ceram. Soc.* **13** (1930) 376.
7. D. S. WILKINSON, *ibid.* **71** (1988) 562.
8. C. E. McNEILLY and G. L. DE POORTER, *Amer. Ceram. Soc. Bull.* **42** (1963) 1.
9. R. PONRAJ and S. RAMAKRISHNA IYER, *J. Mater. Sci. Lett.* **11** (1992) 1000.
10. T. ROUXEL, J. L. BESSON, C. GAULT, P. GOURSAT, M. LEIGH and S. HAMPSHIRE, *ibid.* **8** (1989) 1158.
11. R. PONRAJ and S. RAMAKRISHNA IYER, 46th Annual Technical Meeting, Indian Institute of Metals, Paper No. P/NF. 5.2 (Nov 1992). Udaipur, India.
12. W. D. KINGERY, H. K. BROWEN and D. R. UHLMANN, "Introduction to ceramics" (Wiley, 1976) 704.
13. W. D. CANNON and T. G. LANGDON, *J. Mater. Sci.* **23** (1988) 1.
14. R. F. DAVIS and J. A. PASK, *J. Amer. Ceram. Soc.* **55** (1972) 525.
15. V. M. RADHAKRISHNAN, *J. Mater. Engng. performance* **1** (1992) 123.
16. J. NEWBERGER, A. HAFUER and D. OLTEANN, *J. Brit. Ceram. Soc.* **71** (1972) 89.

Received 11 August 1992
and accepted 3 June 1993